International Journal of Microwave and Wireless Technologies, 2017, 9(4), 805–813.
doi:10.1017/S1759078716000970

RESEARCH PAPER

Rigorous study of propagation in metallic circular waveguide filled with anisotropic metamaterial

HEDI SAKLI[1], MOHAMED YAHIA[1], WYSSEM FATHALLAH[1], JUN WU TAO[2] AND TAOUFIK AGUILI[1]

This paper presents an extension of the formulation of wave propagation in transverse electric (TE) and transverse magnetic (TM) modes in the case of metallic circular waveguides filled with anisotropic metamaterials. The determined higher-order modes have been analyzed and exploited to the design of filters. Among the particularities of anisotropic material, the backward waves can propagate below the cut-off frequency. The numerical results for TE and TM modes have been compared with theoretical predictions. Good agreements were obtained. We analyzed a periodic structure containing waveguides filled with anisotropic metamaterial using the mode-matching technique. By using modal analysis, our approach reduced considerably the computation time compared to HFSS.

Keyword: Anisotropic metamaterials, Backward and forward waves, Circular waveguides, Mode matching, Propagation

Received 13 September 2015; Revised 24 July 2016; Accepted 27 July 2016; first published online 5 January 2017

I. INTRODUCTION

Recently, many researchers have been interested in the guiding devices using metamaterials in some frequency range for their potential novel applications in microwave circuits and radiofrequency (RF) devices such as the patch antennas, waveguide antennas, resonators, the circulators, the insulators, the phase-converters, and the filters. However, there is a lack in the study of the dispersion of anisotropic metamaterials in circular waveguides. The state-of-the-art of these structures can be found in [1–13]. Many studies of guided modes in circular waveguides with isotropic media [14–17] or negative index materials [18, 19] have been presented in the literature.

In this paper, we extended the studies of the transverse electric (TE) and transverse magnetic (TM) modes to circular waveguides filled with anisotropic metamaterials. The proposed study which takes account of the spatial distribution of the permittivity and permeability of the medium is applied to the transverse fields. Then, we discussed the effects of anisotropic parameter on dispersion characteristics. Among the particularities of this anisotropic material, the backward waves can propagate below the cut-off frequency in the guide. The numerical results for TE and TM modes were obtained and compared with theoretical predictions. The design of anisotropic metamaterial circular waveguides discontinuities using mode matching (MM) gave good performances compared to HFSS.

[1]Communication System Laboratory Sys'Com, National Engineering School Of Tunis, University Tunis El Manar, B.P: 37, Le Belvédère, 1002 Tunis, Tunisia
[2]Laboratoire Plasma et Conversion d'Energie LAPLACE, Ecole Nationale Supérieure d'Electrotechnique, d'Electronique, d'Informatique, d'Hydraulique et des Télécommunications, 2 rue Camichel, Toulouse, cedex 31071, France
Corresponding author:
H. Sakli
Email: saklihedi12@gmail.com

II. FORMULATION

In the anisotropic diagonal metamaterials medium, the Maxwell equations are expressed as follows:

$$\vec{\nabla} \times \vec{E} = -j\omega\bar{\bar{\mu}}.\vec{H}, \tag{1}$$

$$\vec{\nabla} \times \vec{H} = j\omega\bar{\bar{\varepsilon}}.\vec{E} \tag{2}$$

with

$$\bar{\bar{\mu}} = \mu_0 \begin{pmatrix} \mu_{rr} & 0 & 0 \\ 0 & \mu_{r\theta} & 0 \\ 0 & 0 & \mu_{rz} \end{pmatrix} = \mu_0 \begin{pmatrix} \mu_{rt} & 0 \\ 0 & \mu_{rz} \end{pmatrix} \tag{3}$$

and

$$\bar{\bar{\varepsilon}} = \varepsilon_0 \begin{pmatrix} \varepsilon_{rr} & 0 & 0 \\ 0 & \varepsilon_{r\theta} & 0 \\ 0 & 0 & \varepsilon_{rz} \end{pmatrix} = \varepsilon_0 \begin{pmatrix} \varepsilon_{rt} & 0 \\ 0 & \varepsilon_{rz} \end{pmatrix}. \tag{4}$$

Let consider a circular waveguide of radius R completely filled with anisotropic metamaterial without losses, as represented in the Fig. 1. The wall of the guide is perfect conductor.

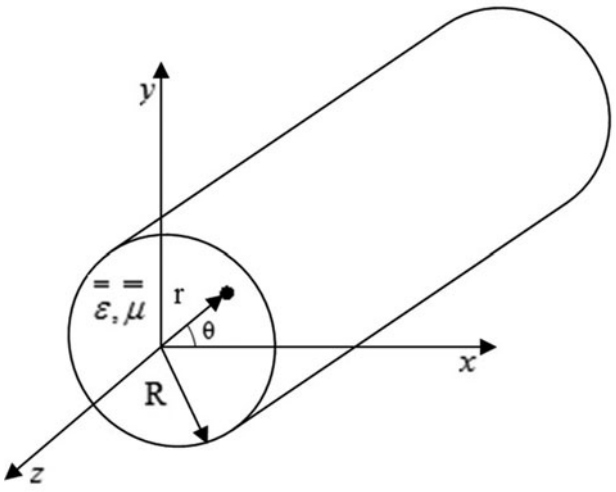

Fig. 1. Geometry of circular waveguide filled with metamaterial.

By considering the propagation in the Oz-direction and manipulating equations (1) and (2), we obtain the expressions of the transverse electromagnetic fields according to the longitudinal fields.

$$E_r = \frac{-j}{K_{c.r}^2}\left(k_z\frac{\partial E_z}{\partial r} + \frac{\omega\mu_o\mu_{r\theta}}{r}\frac{\partial H_z}{\partial\theta}\right), \tag{5}$$

$$E_\theta = \frac{j}{K_{c.\theta}^2}\left(\frac{-k_z}{r}\frac{\partial E_z}{\partial\theta} + \omega\mu_o\mu_{rr}\frac{\partial H_z}{\partial r}\right), \tag{6}$$

$$H_r = \frac{-j}{K_{c.\theta}^2}\left(-\frac{\omega\varepsilon_o\varepsilon_{r\theta}}{r}\frac{\partial E_z}{\partial\theta} + k_z\frac{\partial H_z}{\partial r}\right), \tag{7}$$

$$H_\theta = \frac{j}{K_{c.r}^2}\left(-\omega\varepsilon_o\varepsilon_{rr}\frac{\partial E_z}{\partial r} - \frac{k_z}{r}\frac{\partial H_z}{\partial\theta}\right) \tag{8}$$

with

$$K_{c.r}^2 = k_o^2\varepsilon_{rr}\mu_{r\theta} - k_z^2, \tag{9}$$

$$K_{c.\theta}^2 = k_o^2\varepsilon_{r\theta}\mu_{rr} - k_z^2, \tag{10}$$

$$k_o^2 = \omega^2\varepsilon_o\mu_o. \tag{11}$$

In this paper, we study rigorously the TE and TM modes in this anisotropic waveguide.

A) TE modes

From equation (1), the differential equation for z-component can be obtained as follows:

$$\frac{\partial^2 H_z}{\partial r^2} + \frac{1}{r}\frac{\partial H_z}{\partial r} + \left(\frac{K_{c.\theta}^{(h)}\cdot\sqrt{\mu_{r\theta}}}{K_{c.r}^{(h)}\cdot\sqrt{\mu_{rr}}}\right)^2\frac{1}{r^2}\frac{\partial^2 H_z}{\partial\theta^2} + \left(\frac{\sqrt{\mu_{rz}}}{\sqrt{\mu_{rr}}}K_{c.\theta}^{(h)}\right)^2 H_z = 0. \tag{12}$$

The resolution of the differential equation (12), using the separation of the variables (r,θ), requires the expression of H_z for the TE_{mn} modes in the circular metallic waveguide fully filled of anisotropic metamaterial. The expression of the longitudinal magnetic field can be written as follows:

$$H_z^{(h)} = H_o\sin\left(\frac{K_{c.\theta}^{(h)}\cdot\sqrt{\mu_{r\theta}}}{K_{c.r}^{(h)}\cdot\sqrt{\mu_{rr}}}n.\theta\right)J_n\left(\frac{\sqrt{\mu_{rz}}}{\sqrt{\mu_{rr}}}K_{c.\theta}^{(h)}.r\right)e^{-jk_z z}. \tag{13}$$

J_n is the Bessel function of the first kind of order n ($n = 0, 1, 2, 3,\ldots$).

The expressions (5)–(8) become

$$E_r^{(h)} = \frac{-j\omega\mu_o\mu_{r\theta}}{K_{c.r}^2.r}\left(\frac{K_{c.\theta}^{(h)}\cdot\sqrt{\mu_{r\theta}}}{K_{c.r}^{(h)}\cdot\sqrt{\mu_{rr}}}n.\theta\right)H_o.\cos\left(\frac{K_{c.\theta}^{(h)}\cdot\sqrt{\mu_{r\theta}}}{K_{c.r}^{(h)}\cdot\sqrt{\mu_{rr}}}n.\theta\right).J_n\left(\frac{\sqrt{\mu_{rz}}}{\sqrt{\mu_{rr}}}K_{c.\theta}^{(h)}.r\right)e^{-jk_z z}, \tag{14}$$

$$E_\theta^{(h)} = \frac{j\omega\mu_o\mu_{rr}}{K_{c.\theta}^2}\left(\frac{\sqrt{\mu_{rz}}}{\sqrt{\mu_{rr}}}K_{c.\theta}^{(h)}\right)H_o.\sin\left(\frac{K_{c.\theta}^{(h)}\cdot\sqrt{\mu_{r\theta}}}{K_{c.r}^{(h)}\cdot\sqrt{\mu_{rr}}}n.\theta\right).J_n'\left(\frac{\sqrt{\mu_{rz}}}{\sqrt{\mu_{rr}}}K_{c.\theta}^{(h)}.r\right)e^{-jk_z z}, \tag{15}$$

$$H_r^{(h)} = \frac{-jk_z}{K_{c.\theta}^2}\left(\frac{\sqrt{\mu_{rz}}}{\sqrt{\mu_{rr}}}K_{c.\theta}^{(h)}\right)H_o.\sin\left(\frac{K_{c.\theta}^{(h)}\cdot\sqrt{\mu_{r\theta}}}{K_{c.r}^{(h)}\cdot\sqrt{\mu_{rr}}}n.\theta\right).J_n'\left(\frac{\sqrt{\mu_{rz}}}{\sqrt{\mu_{rr}}}K_{c.\theta}^{(h)}.r\right)e^{-jk_z z}, \tag{16}$$

$$H_\theta^{(h)} = \frac{-jk_z}{K_{c.r}^2.r}\left(\frac{K_{c.\theta}^{(h)}\cdot\sqrt{\mu_{r\theta}}}{K_{c.r}^{(h)}\cdot\sqrt{\mu_{rr}}}n\right)H_o.\cos\left(\frac{K_{c.\theta}^{(h)}\cdot\sqrt{\mu_{r\theta}}}{K_{c.r}^{(h)}\cdot\sqrt{\mu_{rr}}}n.\theta\right).J_n\left(\frac{\sqrt{\mu_{rz}}}{\sqrt{\mu_{rr}}}K_{c.\theta}^{(h)}.r\right)e^{-jk_z z} \tag{17}$$

with J_n' is the derivative of the Bessel function of the first kind of order n ($n = 0, 1, 2, 3,\ldots$).

The boundary conditions are written as follows:

$$E_\theta(r = R) = E_z(r = R) = 0. \tag{18}$$

https://doi.org/10.1017/S1759078716000970 Published online by Cambridge University Press

Consequently, from equation (15), we obtain

$$J'_n\left(\frac{\sqrt{\mu_{rz}}}{\sqrt{\mu_{rr}}}K_{c.\theta}^{(h)}.R\right)=0. \tag{19}$$

This implies

$$u'_{nm}=\frac{\sqrt{\mu_{rz}}}{\sqrt{\mu_{rr}}}K_{c.\theta}^{(h)}.R, \tag{20}$$

where u'_{nm} represents the mth zero ($m=1, 2, 3,\ldots$) of the derivative of the Bessel function J'_n of the first kind of order n.

The constant H_0 is determined by normalizing the power flow down the circular guide.

$$P^{TE}=\int_0^R\int_0^{2\pi}\left(E_r^{(h)}H_\theta^{*(h)}-E_\theta^{(h)}H_r^{*(h)}\right)rdrd\theta=1, \tag{21}$$

where * indicates the complex conjugate.

Equation (21) gives

$$H_0=\frac{K_{c.r}^3}{\sqrt{\omega\mu_0 k_z}}\frac{\sqrt{\mu_{rz}}}{\mu_{r\theta}}N_{nm}^{(h)} \tag{22}$$

with

$$N_{nm}^{(h)}=\frac{1}{\sqrt{\sigma_n/2}.((u'_{nm})^2-n^2)^{1/2}.J_n(u'_{nm})}, \tag{23}$$

$$\sigma_n=\begin{cases}2\pi, & \text{if } n=0,\\ \pi-\dfrac{\sin(4\pi a.n)}{4a.n}, & \text{if } n>0,\end{cases} \tag{24}$$

$$a=\frac{K_{c.\theta}^{(h)}.\sqrt{\mu_{r\theta}}}{K_{c.r}^{(h)}.\sqrt{\mu_{rr}}}. \tag{25}$$

Finally, the propagation constant in TE mode is given by

$$k_{z.nm}^{(TE)}=\pm\sqrt{k_0^2\varepsilon_{r\theta}.\mu_{rr}-\frac{\mu_{rr}}{\mu_{rz}}\left(\frac{u'_{nm}}{R}\right)^2}. \tag{26}$$

The cut-off frequency is written as

$$f_{c.nm}^{(TE)}=\frac{c}{2\pi}\frac{1}{\sqrt{|\varepsilon_{r\theta}\mu_{rz}|}}.\left(\frac{u'_{nm}}{R}\right). \tag{27}$$

We can introduce the following effective permeability and effective permittivity to describe the propagation characteristics of the waveguide modes [6, 7, 13].

$$\mu_{r,eff}^{TE}=\mu_{rr}, \tag{28}$$

$$\varepsilon_{r,eff}^{TE}=\varepsilon_{r\theta}\left(1-\frac{1}{\varepsilon_{r\theta}\mu_{rz}k_0^2}.\left(\frac{u'_{nm}}{R}\right)^2\right). \tag{29}$$

Further, it is observed that:

- $k_z^{TE}=k_0\sqrt{\mu_{r,eff}^{TE}.\varepsilon_{r,eff}^{TE}}\succ 0$, for $\mu_{r,eff}^{TE}\succ 0$ and $\varepsilon_{r,eff}^{TE}\succ 0$;
- $k_z^{TE}=-k_0\sqrt{\mu_{r,eff}^{TE}.\varepsilon_{r,eff}^{TE}}\prec 0$, for $\mu_{r,eff}^{TE}\prec 0$ and $\varepsilon_{r,eff}^{TE}\prec 0$;
- $k_z^{TE}=\pm jk_0\sqrt{\mu_{r,eff}^{TE}.\varepsilon_{r,eff}^{TE}}$, for $\mu_{r,eff}^{TE}.\varepsilon_{r,eff}^{TE}\prec 0$.

The sign of $\varepsilon_{r,eff}^{TE}$ depends on the sign of μ_{rz} as follows:

1) FIRST CASE: $\mu_{rz}\succ 0$

For $\varepsilon_{r\theta}\succ 0$, we have

$$\begin{aligned}\varepsilon_{r,eff}^{TE}&=|\varepsilon_{r\theta}|\left(1-\frac{1}{|\varepsilon_{r\theta}\mu_{rz}|k_0^2}.\left(\frac{u'_{nm}}{R}\right)^2\right)\\&=|\varepsilon_{r\theta}|\left(1-\left(\frac{f_{c.nm}^{TE}}{f}\right)^2\right)\prec 0 \text{ if } f\prec f_{c.nm}^{TE}.\end{aligned} \tag{30}$$

For $\varepsilon_{r\theta}\prec 0$, $\varepsilon_{r,eff}^{TE}$ is rewritten as

$$\varepsilon_{r,eff}^{TE}=-|\varepsilon_{r\theta}|\left(1+\frac{1}{|\varepsilon_{r\theta}\mu_{rz}|k_0^2}.\left(\frac{u'_{nm}}{R}\right)^2\right)\prec 0. \tag{31}$$

It can be seen that $\mu_{rz}\succ 0$ leads to $\varepsilon_{r,eff}^{TE}\prec 0$ below the cut-off frequency whenever $\varepsilon_{r\theta}\succ 0$ or $\varepsilon_{r\theta}\prec 0$.

2) SECOND CASE: $\mu_{rz}\prec 0$

For $\varepsilon_{r\theta}\succ 0$, $\varepsilon_{r,eff}^{TE}$ is rewritten as

$$\varepsilon_{r,eff}^{TE}=|\varepsilon_{r\theta}|\left(1+\frac{1}{|\varepsilon_{r\theta}\mu_{rz}|k_0^2}.\left(\frac{u'_{nm}}{R}\right)^2\right)\succ 0. \tag{32}$$

For $\varepsilon_{r\theta}\prec 0$, we obtain

$$\begin{aligned}\varepsilon_{r,eff}^{TE}&=-|\varepsilon_{r\theta}|\left(1-\frac{1}{|\varepsilon_{r\theta}\mu_{rz}|k_0^2}.\left(\frac{u'_{nm}}{R}\right)^2\right)\\&=-|\varepsilon_{r\theta}|\left(1-\left(\frac{f_{c.nm}^{TE}}{f}\right)^2\right)\succ 0 \text{ if } f\prec f_{c.nm}^{TE}.\end{aligned} \tag{33}$$

Consequently, $\mu_{rz}\prec 0$ leads to $\varepsilon_{r,eff}^{TE}\succ 0$ below the cut-off frequency whenever $\varepsilon_{r\theta}\succ 0$ or $\varepsilon_{r\theta}\prec 0$.

As a result, the sign of the relative effective permittivity of the circular waveguide filled with an anisotropic metamaterial is determined by the relative permeability μ_{rz} below the cut-off frequency. Furthermore, the sign of the propagation constants of the studied waveguide is determined by the sign of the product $\mu_{rr}.\mu_{rz}$ of the metamaterial below the cut-off frequency.

The forward waves are obtained for $\mu_{rz}\prec 0$ and $\mu_{rr}\succ 0$ and backward waves for $\mu_{rz}\succ 0$ and $\mu_{rr}\prec 0$. Therefore, not only backward waves can propagate below the cut-off frequency, but the forward waves can propagate too.

https://doi.org/10.1017/S1759078716000970 Published online by Cambridge University Press

B) TM modes

Similarly to TE modes, TM modes can be derived as follows:

From equation (2), the differential equation for z-component can be obtained

$$\frac{\partial^2 E_z}{\partial r^2}+\frac{1}{r}\frac{\partial E_z}{\partial r}+\left(\frac{K_{c.r}^{(e)}\cdot\sqrt{\varepsilon_{r\theta}}}{K_{c.\theta}^{(e)}\cdot\sqrt{\varepsilon_{rr}}}\right)^2\frac{1}{r^2}\frac{\partial^2 E_z}{\partial\theta^2}+\left(\frac{\sqrt{\varepsilon_{rz}}}{\sqrt{\varepsilon_{rr}}}K_{c.r}^{(e)}\right)^2 E_z=0. \tag{34}$$

The resolution of the differential equation (34), using the separation of the variables (r,θ), requires the expression of E_z for the TM_{nm} modes in the circular metallic waveguide fully filled of anisotropic metamaterial. The expression of the longitudinal electric field can be written as follows:

$$E_z^{(e)}=E_0\cos\left(\frac{K_{c.\theta}^{(e)}\cdot\sqrt{\varepsilon_{rr}}}{K_{c.r}^{(e)}\cdot\sqrt{\varepsilon_{r\theta}}}n.\theta\right)J_n\left(\frac{\sqrt{\varepsilon_{rz}}}{\sqrt{\varepsilon_{rr}}}K_{c.r}^{(e)}.r\right)e^{-jk_z z} \tag{35}$$

The expressions (5)–(8) become

$$E_r^{(e)}=\frac{-jk_z}{K_{c.r}}\frac{\sqrt{\varepsilon_{rz}}}{\sqrt{\varepsilon_{rr}}}E_0.\cos\left(\frac{K_{c.\theta}^{(e)}\cdot\sqrt{\varepsilon_{rr}}}{K_{c.r}^{(e)}\cdot\sqrt{\varepsilon_{r\theta}}}n.\theta\right)J_n'\left(\frac{\sqrt{\varepsilon_{rz}}}{\sqrt{\varepsilon_{rr}}}K_{c.r}^{(e)}.r\right)e^{-jk_z z}, \tag{36}$$

$$E_\theta^{(e)}=\frac{jk_z}{K_{c.\theta}.K_{c.r}}\frac{\sqrt{\varepsilon_{rr}}}{\sqrt{\varepsilon_{r\theta}}}\frac{n}{r}E_0.\sin\left(\frac{K_{c.\theta}^{(e)}\cdot\sqrt{\varepsilon_{rr}}}{K_{c.r}^{(e)}\cdot\sqrt{\varepsilon_{r\theta}}}n.\theta\right)J_n\left(\frac{\sqrt{\varepsilon_{rz}}}{\sqrt{\varepsilon_{rr}}}K_{c.r}^{(e)}.r\right)e^{-jk_z z}, \tag{37}$$

$$H_r^{(e)}=\frac{-j\omega\varepsilon_0}{K_{c.\theta}.K_{c.r}}\sqrt{\varepsilon_{r\theta}}\sqrt{\varepsilon_{rr}}.\frac{n}{r}E_0.\sin\left(\frac{K_{c.\theta}^{(e)}\cdot\sqrt{\varepsilon_{rr}}}{K_{c.r}^{(e)}\cdot\sqrt{\varepsilon_{r\theta}}}n.\theta\right)J_n\left(\frac{\sqrt{\varepsilon_{rz}}}{\sqrt{\varepsilon_{rr}}}K_{c.r}^{(e)}.r\right)e^{-jk_z z}, \tag{38}$$

$$H_\theta^{(e)}=\frac{-j\omega\varepsilon_0}{K_{c.r}}\sqrt{\varepsilon_{rr}}\sqrt{\varepsilon_{rz}}.E_0.\cos\left(\frac{K_{c.\theta}^{(e)}\cdot\sqrt{\varepsilon_{rr}}}{K_{c.r}^{(e)}\cdot\sqrt{\varepsilon_{r\theta}}}n.\theta\right)J_n'\left(\frac{\sqrt{\varepsilon_{rz}}}{\sqrt{\varepsilon_{rr}}}K_{c.r}^{(e)}.r\right)e^{-jk_z z}. \tag{39}$$

The boundary condition (18) gives the following equation:

$$J_n(u_{nm})=0 \tag{40}$$

with

$$u_{nm}=\frac{\sqrt{\varepsilon_{rz}}}{\sqrt{\varepsilon_{rr}}}K_{c.r}^{(e)}.R. \tag{41}$$

In equation (41) u_{nm} represents the mth zero ($m=1, 2, 3, \ldots$) of the Bessel function J_n of the first kind of order n.

The constant E_0 is determined by normalizing the power flow down the circular guide.

$$P^{TM}=\int_0^R\int_0^{2\pi}\left(E_r^{(e)}H_\theta^{*(e)}-E_\theta^{(e)}H_r^{*(e)}\right)rdrd\theta=1. \tag{42}$$

Equation (42) gives:

$$E_0=\frac{K_{c.r}^2}{\sqrt{\omega\varepsilon_0\varepsilon_{rr}k_z}}N_{nm}^{(e)} \tag{43}$$

with

$$N_{nm}^{(e)}=\frac{1}{u_{nm}.J_n'(u_{nm}).\sqrt{\delta_n/2}}, \tag{44}$$

$$\delta_n=\begin{cases}2\pi, & \text{if } n=0,\\ \pi-\dfrac{\sin(4\pi b.n)}{4b.n}, & \text{if } n>0,\end{cases} \tag{45}$$

$$b=\frac{K_{c.\theta}^{(e)}\cdot\sqrt{\varepsilon_{rr}}}{K_{c.r}^{(e)}\cdot\sqrt{\varepsilon_{r\theta}}}. \tag{46}$$

Finally, the propagation constant in TM mode is given by:

$$k_{z.nm}^{(TM)}=\pm\sqrt{k_0^2\varepsilon_{rr}.\mu_{r\theta}-\frac{\varepsilon_{rr}}{\varepsilon_{rz}}\left(\frac{u_{nm}}{R}\right)^2}. \tag{47}$$

Obviously, the cut-off frequency is written

$$f_{c.nm}^{(TM)}=\frac{c}{2\pi}\frac{1}{\sqrt{|\mu_{r\theta}\varepsilon_{rz}|}}.\left(\frac{u_{nm}}{R}\right). \tag{48}$$

We can introduce the following effective permeability and effective permittivity to describe the propagation characteristics of the waveguide modes.

$$\varepsilon_{r,eff}^{TM}=\varepsilon_{rr}, \tag{49}$$

$$\mu_{r,eff}^{TM}=\mu_{r\theta}\left(1-\frac{1}{\mu_{r\theta}\varepsilon_{rz}k_0^2}.\left(\frac{u_{nm}}{R}\right)^2\right). \tag{50}$$

Similar to the previous discussion, we have three possibilities:

Further, it is observed that:

- $k_z^{TM}=k_0\sqrt{\mu_{r,eff}^{TM}.\varepsilon_{r,eff}^{TM}}\succ 0$, for $\mu_{r,eff}^{TM}\succ 0$ and $\varepsilon_{r,eff}^{TM}\succ 0$,
- $k_z^{TM}=-k_0\sqrt{\mu_{r,eff}^{TM}.\varepsilon_{r,eff}^{TM}}\prec 0$, for $\mu_{r,eff}^{TM}\prec 0$ and $\varepsilon_{r,eff}^{TM}\prec 0$,
- $k_z^{TM}=\pm jk_0\sqrt{\mu_{r,eff}^{TM}.\varepsilon_{r,eff}^{TM}}$, for $\mu_{r,eff}^{TM}.\varepsilon_{r,eff}^{TM}\prec 0$.

Consequently, the sign of $\mu_{r,eff}^{TM}$ depends on the sign of ε_{rz} as follows:

https://doi.org/10.1017/S1759078716000970 Published online by Cambridge University Press

1) CASE WHEN $\varepsilon_{rz} \succ 0$

In this case, for $\mu_{r\theta} \succ 0$, $\mu_{r,eff}^{TM}$ is rewritten as

$$\mu_{r,eff}^{TM} = |\mu_{r\theta}|\left(1 - \frac{1}{|\mu_{r\theta}\varepsilon_{rz}|k_0^2}.\left(\frac{u_{nm}}{R}\right)^2\right) = |\mu_{r\theta}|\left(1 - \left(\frac{f_{c.nm}^{TM}}{f}\right)^2\right) \prec 0 \text{ if } f \prec f_{c.nm}^{TM}. \quad (51)$$

For $\mu_{r\theta} \prec 0$, we have

$$\mu_{r,eff}^{TM} = -|\mu_{r\theta}|\left(1 + \frac{1}{|\mu_{r\theta}\varepsilon_{rz}|k_0^2}.\left(\frac{u_{nm}}{R}\right)^2\right) \prec 0. \quad (52)$$

It can be seen that $\varepsilon_{rz} \succ 0$ leads to $\mu_{r,eff}^{TM} \prec 0$ below the cut-off frequency whenever $\mu_{r\theta} \succ 0$ or $\mu_{r\theta} \prec 0$.

2) CASE WHEN $\varepsilon_{rz} \prec 0$

In this case, for $\mu_{r\theta} \succ 0$, we have

$$\mu_{r,eff}^{TM} = |\mu_{r\theta}|\left(1 + \frac{1}{|\mu_{r\theta}\varepsilon_{rz}|k_0^2}.\left(\frac{u_{nm}}{R}\right)^2\right) \succ 0. \quad (53)$$

For $\mu_{r\theta} \prec 0$, we obtain

$$\mu_{r,eff}^{TM} = -|\mu_{r\theta}|\left(1 - \frac{1}{|\mu_{r\theta}\varepsilon_{rz}|k_0^2}.\left(\frac{u_{nm}}{R}\right)^2\right) = -|\mu_{r\theta}|\left(1 - \left(\frac{f_{c.nm}^{TM}}{f}\right)^2\right) \succ 0 \text{ if } f \prec f_{c.nm}^{TM}. \quad (54)$$

It is also seen that the sign of $\mu_{r,eff}^{TM}$ is determined by ε_{rz} which is independent of $\mu_{r\theta}$. The wave propagates in the form of a forward wave in the waveguide for $\varepsilon_{rz} \prec 0$ and $\varepsilon_{rr} \succ 0$, and the wave propagates in the form of a backward wave for $\varepsilon_{rz} \succ 0$ and $\varepsilon_{rr} \prec 0$.

According to this analysis, it is found that both the forward waves and the backward waves are possible in any frequency region. This is determined by the sign of μ_{rz} and μ_{rr} for TE modes and by the sign of ε_{rz} and ε_{rr} for TM modes. Therefore, we observe that in addition to backward waves, the forward waves can propagate below the cut-off frequency.

C) Analysis of uni-axial discontinuities in the circular waveguides

In this section, we extended the use of MM to characterize uni-axial discontinuities between circular waveguides filled with the studied medium. The discontinuities are considered without losses. This method based on the modal development of the transverse electromagnetic fields.

We consider in Fig. 2 a junction between two circular waveguides filled with two different media having the same cross-section where a^i and b^i are the incident and the reflected waves, respectively.

The TE and magnetic fields (E_T, H_T) in the wave guides can be written in the modal bases as follows [20]:

$$E_T = \sum_{m=1}^{\infty} A_m^i\left(a_m^i + b_m^i\right)e_m^i, \quad (55)$$

$$H_T = \sum_{m=1}^{\infty} B_m^i\left(a_m^i - b_m^i\right)h_m^i, \quad (56)$$

where E_T and H_T are the TE and magnetic fields (the sub-index T refers to the components in the transverse plane) A_m^i and B_m^i are complex coefficients which are determined by normalizing the power flow down the circular guides ($i = I$, II and m is the index of the mode). e_m^i, h_m^i represent the mth electric and magnetic modal eigenfunction in the guide i, respectively.

At the junction, the continuity of the fields allows to write the following equations:

$$E_t^I = E_t^{II}, \quad (57)$$

$$H_t^I = H_t^{II}. \quad (58)$$

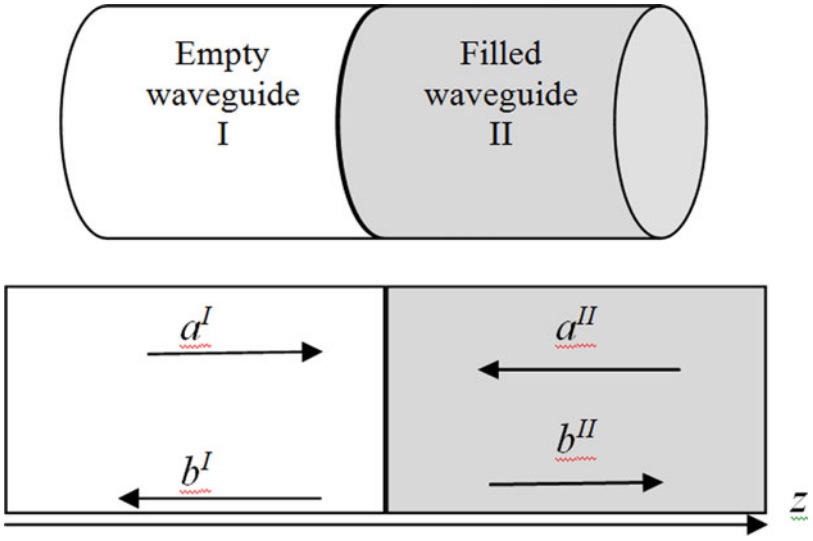

Fig. 2. Junction between two circular waveguides filled with two different media having the same cross-section.

https://doi.org/10.1017/S1759078716000970 Published online by Cambridge University Press

By postponing the equations (55) and (56) in (57) and (58), we obtain:

$$\sum_{m=1}^{N_1} A_m^I\left(a_m^I + b_m^I\right)e_m^I = \sum_{p=1}^{N_2} A_p^{II}\left(a_p^{II} + b_p^{II}\right)e_p^{II}, \tag{59}$$

$$\sum_{m=1}^{N_1} B_m^I\left(a_m^I - b_m^I\right)h_m^I = \sum_{p=1}^{N_2} B_p^{II}\left(-a_p^{II} + b_p^{II}\right)h_p^{II}. \tag{60}$$

N_1 and N_2 are the number of considered modes in guides 1 and 2, respectively. By applying the Galerkin's method, equations (59) and (60), lead to the following systems:

$$\sum_{m=1}^{N_1} A_m^I\left(a_m^I + b_m^I\right)\langle e_m^I|e_p^{II}\rangle = A_p^{II}\left(a_p^{II} + b_p^{II}\right), \tag{61}$$

$$B_m^I\left(a_m^I - b_m^I\right) = \sum_{p=1}^{N_2} B_p^{II}\left(-a_p^{II} + b_p^{II}\right)\langle h_p^{II}|h_m^I\rangle. \tag{62}$$

The inner product is defined as:

$$\langle e_m|e_p\rangle = \int_S e_m^* e_p\, dS. \tag{63}$$

Equations (61) and (62) give:

$$-a_p^{II} + \sum_{m=1}^{N_1}\frac{A_m^I}{A_p^{II}}a_m^I\langle e_m^I|e_p^{II}\rangle = b_p^{II} - \sum_{m=1}^{N_1}\frac{A_m^I}{A_p^{II}}b_m^I\langle e_m^I|e_p^{II}\rangle, \tag{64}$$

$$a_m^I + \sum_{p=1}^{N_2}\frac{B_p^{II}}{B_m^I}a_p^{II}\langle h_p^{II}|h_m^I\rangle = b_m^I + \sum_{p=1}^{N_2}\frac{B_p^{II}}{B_m^I}b_p^{II}\langle h_p^{II}|h_m^I\rangle, \tag{65}$$

which can be written in matrix form:

$$\begin{bmatrix} U & M_1 \\ M_2 & -U \end{bmatrix}\begin{bmatrix} a_1^I \\ . \\ a_{N_1}^I \\ a_1^{II} \\ . \\ a_{N_2}^{II} \end{bmatrix} = \begin{bmatrix} U & M_1 \\ -M_2 & U \end{bmatrix}\begin{bmatrix} b_1^I \\ . \\ b_{N_1}^I \\ b_1^{II} \\ . \\ b_{N_2}^{II} \end{bmatrix} \tag{66}$$

where U is the identity matrix. M_1 and M_2 are defined as:

$$M_{1ij} = \frac{B_j^{II}}{B_i^I}\langle h_j^{II}|h_i^I\rangle, \tag{67}$$

$$M_{2ij} = \frac{A_i^I}{A_j^{II}}\langle e_i^I|e_j^{II}\rangle. \tag{68}$$

The scattering matrix of the discontinuity is:

$$S = \begin{bmatrix} U & M_1 \\ -M_2 & U \end{bmatrix}^{-1}\begin{bmatrix} U & M_1 \\ M_2 & -U \end{bmatrix}. \tag{69}$$

For a structure having cascaded uni-axial discontinuities, the total scattering matrix is obtained by chaining the S scattering matrices of all discontinuities [21].

III. NUMERICAL RESULTS AND DISCUSSION

A) Propagating modes

In the first stage, we study the TE modes of metallic circular waveguide of radius $R = 13.4$ mm fully filled with an anisotropic metamaterials (see Fig. 1) having negative μ_{rz} or negative μ_{rr}. The resonant frequency of the fundamental mode of the equivalent empty circular waveguide is 6.57 GHz. For the case of isotropic metamaterial with a permittivity $\varepsilon_r = -4.4$ and a permeability $\mu_r = -1$, the resonant frequency of the fundamental mode is $f_{c.11}^{TE} = 3.13$ GHz.

Figure 3 represents the curves of the propagation constant for the first five TE modes and for frequency range 1–10 GHz, $\mu_{rr} = 1$, $\mu_{rz} = -1$, and $\varepsilon_{r\theta} = 4.4$. All modes propagate without cut-off frequencies (forward waves). Figure 4 displays the same diagrams for $\mu_{rr} = -1$, $\mu_{rz} = 1$, and $\varepsilon_{r\theta} = 4.4$. When n and m is small and ω is large, the waves stop propagating. Therefore, these modes propagate at low frequencies and cutoff at high frequencies (backward waves).

It is interesting to see that by controlling the signs of μ_{rz} and μ_{rr}, both forward and backward waves can be obtained. Figures 3 and 4 show that our results agree well with the predicted ones.

Let consider now the TM modes. Figure 5 represents the curves of propagation constant for the first five TM modes and for the frequency range is 1–10 GHz, and $\varepsilon_{rr} = 4.4$, $\varepsilon_{rz} = -4.4$, $\mu_{r\theta} = 1$. All modes propagate without cutoff (forward waves). Figure 6 represents a calculated curves of

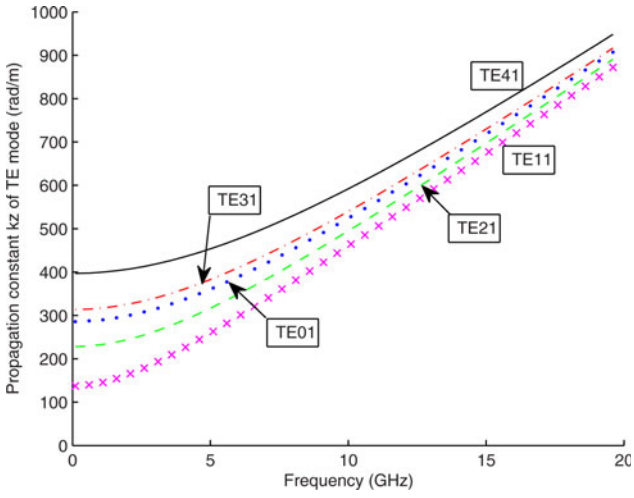

Fig. 3. Curves of propagation constant k_z^{TE} for TE mode of the circular waveguide completely filled anisotropic metamaterial with parameters $\mu_{rr} = 1$, $\mu_{rz} = -1$, $\varepsilon_{r\theta} = 4.4$.

https://doi.org/10.1017/S1759078716000970 Published online by Cambridge University Press

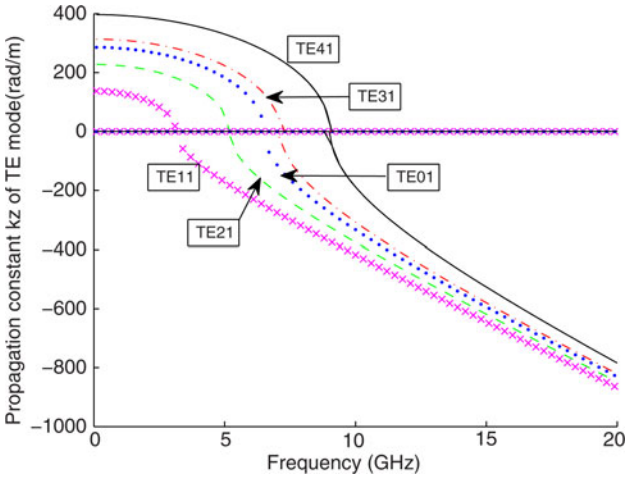

Fig. 4. Curves of propagation constant k_z^{TE} for TE mode of the circular waveguide completely filled anisotropic metamaterial with parameters $\mu_{rr} = -1$, $\mu_{rz} = 1$, $\varepsilon_{r\theta} = 4.4$.

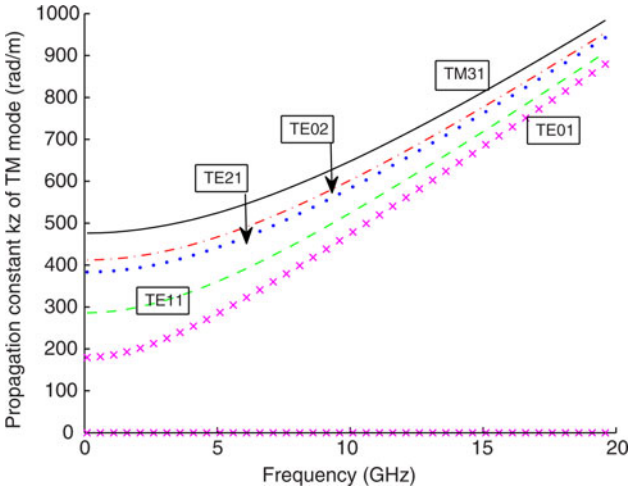

Fig. 5. Curves of propagation constant k_z^{TM} for TM mode of the circular waveguide completely filled anisotropic metamaterial with parameters $\varepsilon_{rr} = 4.4$, $\varepsilon_{rz} = -4.4$, $\mu_{r\theta} = 1$.

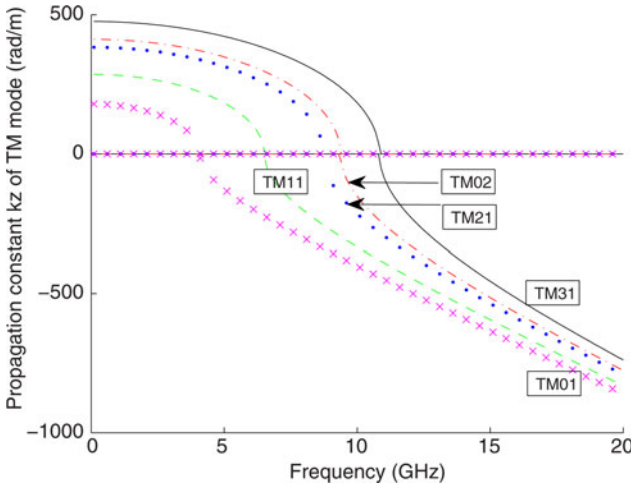

Fig. 6. Curves of propagation constant k_z^{TM} for TM mode of the circular waveguide completely filled anisotropic metamaterial with parameters $\varepsilon_{rr} = -4.4$, $\varepsilon_{rz} = 4.4$, $\mu_{r\theta} = 1$.

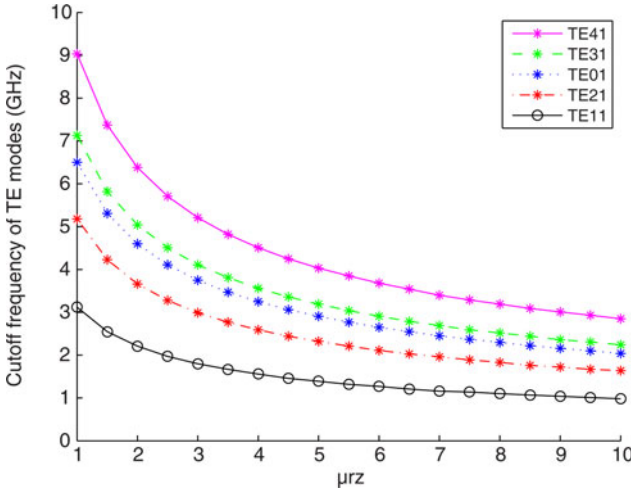

Fig. 7. Cut-off frequencies for the first five TE modes versus μ_{rz} with $\mu_{rr} = -1$, $\varepsilon_{r\theta} = 4.4$.

propagation constant for the first five TM modes and for the frequency range is 1–10 GHz, and $\varepsilon_{rr} = -4.4$, $\varepsilon_{rz} = 4.4$, $\mu_{r\theta} = 1$.

We notice that by controlling the signs of ε_{rz} and ε_{rr}, both forward wave and backward wave can be obtained. Figures 5 and 6 show that our results agree well with the predicted ones.

In Fig. 7, for $\mu_{rr} = -1$ and $\varepsilon_{r\theta} = 4.4$. We observe that the cut-off frequencies of lowest TE modes decreased with the respect increase of μ_{rz}. In a same manner in Fig. 8, for $\varepsilon_{rr} = -4.4$ and $\mu_{r\theta} = 1$, the TM cut-off frequencies decreased with the respect increase of ε_{rz}. Consequently, the propagating mode can be controlled by varying the parameters of material.

B) Filter design

We consider now, 12 discontinuities (see Fig. 9) constituted by juxtaposing 13 circular waveguides having the same dimensions ($R = 13.4$ mm). The circuit is formed by alternation of empty guide ($\varepsilon_r = \mu_r = 1$) of width $l = 10$ mm and guide

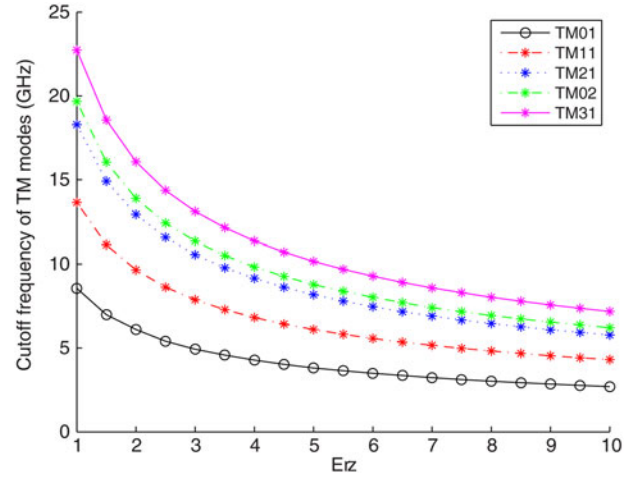

Fig. 8. Cut-off frequencies for the first five TM mode versus ε_{rz} with $\varepsilon_{rr} = -4.4$, $\mu_{r\theta} = 1$.

https://doi.org/10.1017/S1759078716000970 Published online by Cambridge University Press

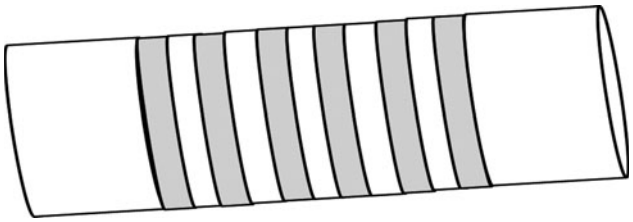

Fig. 9. Geometry of the circular waveguide with 12 discontinuities.

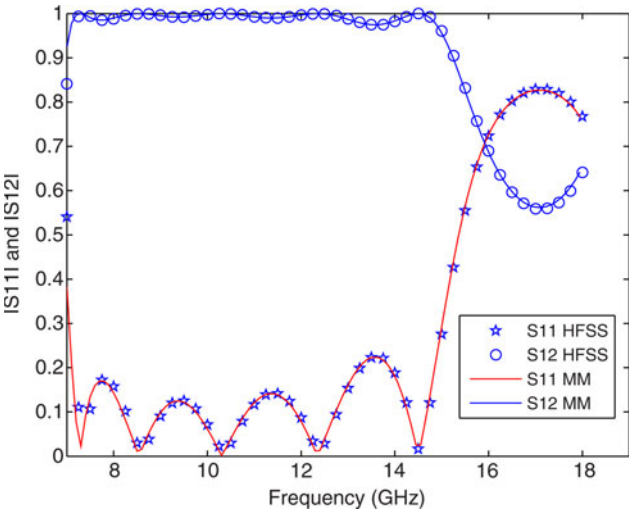

Fig. 10. Reflection Coefficient of the periodic structure with 12 discontinuities.

filled by anisotropic metamaterials ($\varepsilon_{rr} = \varepsilon_{r\theta} = -\varepsilon_{rz} = -4.4$; $\mu_{rr} = \mu_{r\theta} = -\mu_{rz} = 1$) of width $d = 0.2$ mm (periodic structure). Figure 9 represents the geometry of the studied structure.

Figure 10 represents the response circuit in terms of reflection and transmission coefficients as a function of the frequency using our approach and HFSS. For the modal method, we used eight modes in the whole circuit. We note that both simulations are in perfect agreement. However, our method is significantly faster than HFSS especially if the number of discontinuities increases. Then, by using our approach, it could easy to design band-pass or low-pass filters according to a given specifications.

VI. CONCLUSION

Rigorous TE and TM modes analysis of circular anisotropic metamaterial waveguides has been developed. It was demonstrated that the electromagnetic characteristics of the waveguide are closely dependent on constitutive parameters of the filled metamaterial. The curves of dispersion of the fundamental mode and the first four higher-order modes of the metamaterial waveguide are obtained by using Matlab.

We found that both the forward and the backward waves are possible in different frequency ranges below and above the cut-off frequency. This is determined by the sign of μ_{rz} and μ_{rr} for TE modes and by the sign of ε_{rz} and ε_{rr} for TM modes. Our results are in good agreement with the theoretical prediction.

Moreover, in this paper, we applied the MM technique to analyze multiple uni-axial discontinuities in circular metallic waveguides filled with anisotropic metamaterials. This introduced tool is applied to the modeling of large complex structures such as filters where its rapidity compared with the commercial simulation tools is verified. The proposed formulation can be a useful tool for engineers of microwave.

REFERENCES

[1] Alu, A.; Engheta, N.: Mode excitation by a line source in a parallel plate waveguide filled with a pair of parallel double-negative and double-positive slabs, in IEEE AP-S Int. Symp., Columbus, OH, 2003, 359–362.

[2] Xu, Y.: Wave propagation in rectangular waveguide filled with single negative metamaterial slab. IEE Electron. Lett., **39** (25) (2003), 1831–1833.

[3] Xu, Y.: A study of waveguides field with anisotropic metamaterials. Microw. Opt. Technol. Lett., **41** (2004), 426–431.

[4] Alu, A.; Engheta, N.: Guided modes in a waveguide filled with a pair of single-negative (SNG), double negative (DNG), and/or double-positive (DPS) layers. IEEE Trans. Microw. Theory Tech., **52** (2004), 199–210.

[5] Cory, H.; Shtrom, A.: Wave propagation along a rectangular metallic waveguide longitudinally loaded with a metamaterial slab. Microw. Opt. Technol. Lett., **41** (2) (2004), 123–127.

[6] Meng, F.Y.; Wu, Q.; Fu, J.H.; Gu, X.M.; Li, L.W.: Transmission characteristics of wave modes in a rectangular waveguide filled with anisotropic metamaterial. Appl. Phys. A, **94** (2009), 747–753.

[7] Meng, F.Y.; Wu, Q.; Li, L.W.: Controllable metamaterial-loaded waveguides supporting backward and forward waves transmission characteristics of wave modes in a rectangular waveguide filled with anisotropic metamaterial. IEEE Trans. Antennas Propag., **59** (9) (2011), 3400–3411.

[8] Zhang, D.; Ma, J.: The propagation and cutoff frequencies of the rectangular metallic waveguide partially filled with metamaterial multilayer slabs. Progr. Electromagn. Res. M, **9** (2009), 35–40.

[9] Pan, Y.; Xu, S.: Cpmlex modes in parallel-plate waveguide structure filled with left-handed material. Chin. J. Electron., **18** (3) (2009), 551–554.

[10] Cojocaru, E.: Waveguides filled with bilayers of double-negative (DNG) and double-positive (DPS) metamaterials. Progr. Electromagn. Res. B, **32** (2011), 75–90.

[11] Fathallah, W.; Sakli, H.; Aguili, T.: Electromagnetic wave propagation in anisotropic metamaterial waveguides. JNM, Int. J. Numer. Modell, **28** (2015), 479–486.

[12] Fathallah, W.; Sakli, H.; Aguili, T.: Full-wave study of rectangular metamaterial waveguides using Galerkin's method, in 8th Int. Multi-Conf. on Systems, Signals and Devices, SSD'13, Hammamet, Tunisia, March 2013.

[13] Marques, R.; Martel, J.; Mesa, F.; Medina, F.: Left-handed-media simulation and transmission of EM waves in subwavelength split-ring-resonator-loaded metallic waveguides. Phys. Rev. Lett., **89** (2002), 183901.

[14] Balanis, C.A.: "Circular Waveguides", Material in Advanced Engineering Electromagnetics, Wiley, New York, 1989, Sect. 9.2, 643–650.

[15] Boyenga, D.L.; Mabika, C.N.; Diezaba, A.: A new multimodal variational formulation analysis of cylindrical waveguide uniaxial discontinuities. Res. J. Appl. Sci., Eng. Technol., **6** (5) (2013), 787–792.

https://doi.org/10.1017/S1759078716000970 Published online by Cambridge University Press

[16] Thabet, R.; Riabi, M.L.; Belmeguenai, M.: Rigorous design and efficient optimization of quarter-wave transformers in metallic circular waveguides using the mode-matching method and the genetic algorithm. Progr. Electromagn. Res., **68** (2007), 15–33.

[17] Mahmoud, S.F.: Guided modes on open chirowaveguides. IEEE Trans. Microw. Theory Tech., **43** (1) (1995), 205–209.

[18] Shadrivov, I.V.; Sukhorukov, A.A.; Kivshar, Y.S.: Guided modes in negative-refractive-index waveguides. Phys. Rev. E, **67** (2003), 057602.

[19] Dong, J.-F.; Li, J.: Characteristics of guided modes in uniaxial chiral circular waveguides. Progr. Electromagn. Res., **124** (2012), 331–345.

[20] Couffignal, P.: Contribution à l'étude des filters en guides métalliques. Thesis, INP, Toulouse, France, 1992.

[21] Fathallah, W.; Sakli, H.; Aguili, T.: Scattering matrix analysis of uniaxial anisotropic waveguide discontinuities. IRECAP, Int. J. Commun. Antenna Propag., **4** (3) (2014), 87–93..

Hedi Sakli is born in Tunisia in 1966. He received the M.S. degree in High Frequency Communication Systems from Marne-La-Valley University, France in 2002, a Ph.D. degree in 2009 and HDR degree in 2014 in telecommunications from the National Engineering School of Tunis, Tunis El Manar University, Tunisia. He is since 2010 assistant professor at the University of Gabes. He is the author of more than 30 articles. His research interests propagation in anisotropic media, Ferrite and metamaterials, numerical methods in electromagnetics and antennas.

Mohamed Yahia is born in Tunisia in 1976. He received the M.S. degree in Electronics from Tunis El Manar University, Tunisia in 2004, a Ph.D. degree in 2010 in Electrical Engineering from the National Engineering School of Gabes, Gabes University, Tunisia. Since 2011 he has been 2011 an Assistant Professor at the University of Gabes. He is the author of more than 15 articles. His research interests propagation in waveguide discontinuities, numerical methods in electromagnetic, Filters and antennas.

Wyssem Fathallah is born in Tunisia in 1978. He received the M.S. degree in Micro-Electronics from Monastir University, Tunisia in 2005, a Ph.D. degree in 2015 in Telecommunications from the National Engineering School of Tunis, Tunis El Manar University, Tunisia. Since 2015 he has been 2011 an Assistant Professor at the University of Kirouen, Tunisia. He is the author of more than ten articles. His research interests propagation in anisotropic media, metamaterials, numerical methods in electromagnetics and waveguides.

Jun Wu Tao was born in Hubei, China, in 1962. He received the B.Sc. degree in Electronics from the Radio Engineering Department, Huazhong (Central China) University of Science and Technology, Wuhan, China, in 1982, the Ph.D. degree (with honors) from the Institut National polytechnique of Toulouse, France in 1988, and the Habilitation degree from the University of Savoie, France in 1999. Since September 2001 he is a full position professor at the Institut National Polytechnique of Toulouse where he is involved in the numerical methods for electromagnetics, microwave and RF components design, microwave and millimeter-wave measurements.

Taoufik Aguili was born in Tinis, Tunisia. He received his Dip. Ing. in Electrical Engineering, and Ph.D. degree in Telecommunications from INSA, France. He is working as Professor at Ecole Nationale d"Ingénieurs de Tunis (ENIT). His research activities include electromagnetic microwave circuits modeling and analysis of scattering and propagation phenomena in free space.

https://doi.org/10.1017/S1759078716000970 Published online by Cambridge University Press